Hindawi
International Journal of Antennas and Propagation
Volume 2021, Article ID 5541197, 9 pages
https://doi.org/10.1155/2021/5541197

Research Article

A Bending Passive RFID Tag as a Sensor for High-Temperature Exposure

Zahangir Khan, Xiaochen Chen, Han He, Adnan Mehmood, and Johanna Virkki

Faculty of Medicine and Health Technology (MET), Tampere University, Tampere 33720, Finland

Correspondence should be addressed to Zahangir Khan; zahangir.khan@tuni.fi

Received 5 January 2021; Revised 27 March 2021; Accepted 12 April 2021; Published 22 April 2021

Academic Editor: Rodolfo Araneo

This paper introduces a prototype of a low-energy high-temperature exposure sensor, which is a temperature-sensitive passive UHF RFID tag that bends forward when exposed to warm air. This "Bending Tag" design is based on a simple dipole antenna fabricated from an electro-textile material. The antenna has a 3D-printed substrate, which is constructed from a commercial Thermo Reactive Filament that gets soft when exposed to 50°C for 30 seconds, causing the tag to bend forward and curve. The sensor tag initially has a read range of more than 6 meters throughout the global UHF RFID frequency band. After bending, there is a significant decrease in the read range (to around 2–3 meters), which is caused by the changed backscattered power of the sensor tag. In an office environment, the backscattered power changes from −36 dBm to −43 dBm. The change in a sensor tag-reference tag system as dP% is approximately 70%. Based on these initial results, our bending tag can be further developed to work as a cost-effective low-energy sensor for monitoring high-temperature exposure.

1. Introduction

RFID is a system where the automatic identification of remote objects can be done. Any arbitrary RFID system is generally comprised of three main components, i.e., a reader antenna, a tag, and a system where the communication between the two components is maintained [1–3]. Passive radio frequency identification (RFID) tags have been useful in the commercial context due to their attribute of not requiring a separate power source for operation, making them low cost and easy to manufacture [4]. Passive tags obtain their power from the signal provided by the reader, and the communication between the reader and the tag antenna is done by a method called backscattering [5].

A passive RFID system has been traditionally used for applications involving inventory management, logistics, and personnel identification. However, passive RFID technology is capable of expanding beyond its traditional identification-based applications. It can be utilized to perform as wireless sensors, which are easy to manufacture, low cost, and efficient [3, 6–8]. Adding sensing capabilities to passive RFID tags has been widely studied [9–14], and by tracking changes in the tags' backscattered signals, passive UHF RFID tags have been used for sensing without external sensors, such as strain [15–19], moisture [20–24], pressure [25, 26], and especially temperature sensors [27–29].

Advancements in 3D printing technology have enabled the possibility of manufacturing complex structures with relative ease and low cost. Recent studies involving a combination of 3D printing with RFID technology have led to the development of specific 3D-printed antenna layouts and substrate structures [30–32]. Although 3D printing has been revolutionary in the field of manufacturing, 3D-printed materials usually remain static after being printed. However, it has recently been presented that some materials exhibit physical or structural changes even after the 3D printing process is completed when exposed to certain stimuli over time. This concept of printing is known as 4D printing. The additional dimension, time, is the effect of the exposure of the finished 3D-printed material to certain stimuli, such as moisture, temperature, or light, in a controlled manner.

The application of stimuli can change the characteristics or functionality of the 3D-printed object [33–35].

Previously, for example, Nitinol compound has been demonstrated to be suitable for integration into UHF tags due to its response to temperature variation, which seems to be stable, especially at high temperatures [36]. In general, the application of shape memory alloy in antennas is drawing more research attention [37]. In this study, a 4D-printed passive RFID-based temperature exposure sensor tag is developed. The antenna of the sensor tag was developed using a flexible copper textile, while the sensing part of the tag sensor was developed using a 3D-printed Thermo Reactive Filament (TRF). When exposed to 50°C for 30 seconds, the sensor tag underwent a change in shape, which affected the backscattered signal strength. Furthermore, the integrated reference tag held a stable wireless performance during the bending of the sensor tag. Thus, we can avoid the effects of reflections or external disturbances on the sensor performance, which will make our sensor tag functional at different distances and in different environments. Such a sensor tag-reference tag system has been used, for example, in [19, 38–39]. To the best of our knowledge, this is the first 4D-printed passive RFID-based temperature exposure sensor tag with a referenced readout.

2. Materials and Methods

2.1. 3D-Printed Substrate Preparation. For this experiment, the Thermo Reactive Filament (TRF 45) manufactured by Unitika Ltd. was used to prepare the sensor substrate. The filament is made of a special polyester. After the 3D printing process, the printed structure softens when exposed to a temperature above 45°C. It is in this state that the printed structure can be further molded into any other shape from the original shape after 3D printing. Upon cooling (i.e., when cooled to below 45°C), the 3D-printed structure hardens [40].

The printer used for the 3D printing process is the Prenta Duo XL 3D printer. The substrate that was printed is a 170 mm × 5 mm × 2 mm substrate. It was printed at a temperature of 210°C with an infill density of 100% and with a printing speed of 10 mm/s. The height of the individual layers is 0.1 mm. To ease the printing process, Kapton (polyamide film) was used, which acted as a base substrate for support purposes only. The TRF filament appears to print much more smoothly on Kapton, and the removal of the printed substrate is easier after the printing process. The printing process is as presented in Figure 1.

2.2. Sensor Tag Antenna and Reference Tag Antenna Manufacture. The tag antenna that was used for this experiment is a dipole antenna, which is shown in Figure 2. It was selected for its simplistic design, good read range (7.5 meters in air), and its relative ease of manufacture, and it has been presented earlier in [41]. In this study, the dipole has a uniform electro-textile conductor. The length of the dipole can be adjusted to achieve inductive input impedance to conjugate-match the antenna to an RFID IC.

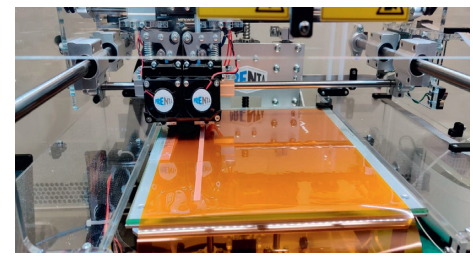

Figure 1: 3D printing of the TRF filament on polyamide film.

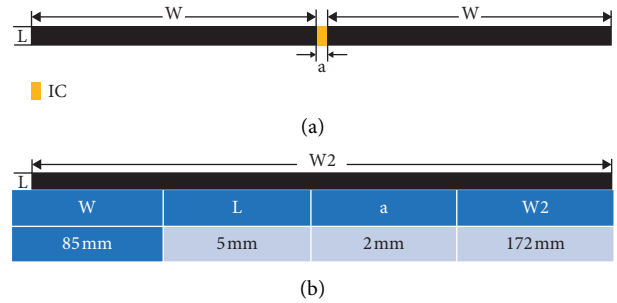

W	L	a	W2
85 mm	5 mm	2 mm	172 mm

(b)

Figure 2: Design of the bending tag antenna (a) and the 3D-printed substrate (b).

The material used for the development of the tag antenna is nonstretchable but highly flexible copper-plated polyester textile (less EMF Cat. #A1212, surface resistivity: 0.05 ohm/sq, and thickness: 0.08 mm). The material was cut manually in accordance with the dimensions shown in Figure 1. An NXP UCODE G2iL series RFID IC (Integrated Circuit) with a wake-up power of −18 dBm (15.8 μW) was attached to the antenna using Loctite Super Glue Precision, a transparent and strong adhesive. In this manner, two tag antennas were first prepared and used as reference tags. For the sensor tag manufacture, the developed 3D-printed substrate was attached to the tag antenna using textile glue, namely, Prym Textil+. In this manner, five sensor tags were prepared. The complete tag structure after the RFID IC attachment is presented in Figure 3.

2.3. Measurements. The 3D-printed substrate was observed under the microscope. After the initial observation, the substrate was placed within an oven and exposed to 50°C for 30 seconds, causing it to soften and bend. After the bent substrate was cooled, it was again observed under the microscope.

The wireless performance of the Bending Tag was first evaluated within an anechoic chamber by the Voyantic Tagformance RFID measurement system. The system consists of an RFID reader with an adjustable output power of up to 30 dBm and an adjustable frequency range of 800–1,000 MHz. It also provides the tag's backscattered signal strength, whose lowest power rating is −80 dBm. Initially, a reference tag is used to calibrate the reader antenna of the system and the position of the tag to be measured. The theoretical read range between the tag and the reader antenna is based on the measured path loss and threshold power:

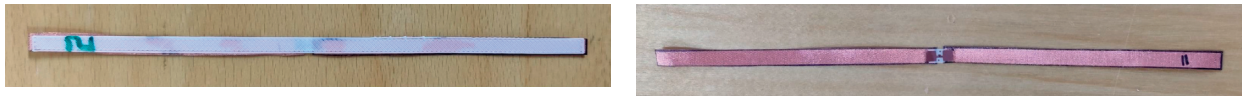

(a) (b)

Figure 3: A ready-made bending tag: 3D-printed substrate side (a) and tag antenna side (b). The thickness of the 3D-printed layer is 0.2 mm and the thickness of the antenna is 0.08 mm.

$$d_{\text{Tag}} = \frac{\lambda}{4\pi}\sqrt{\frac{\text{EIRP}}{P_{\text{TS}}\,L_{\text{fwd}}}}, \tag{1}$$

where EIRP is the emission limit of an RFID reader, given as the equivalent isotropic radiated power. In this study, EIRP = 3.28 W, which is the emission limit in European countries. The wavelength transmitted from the reader antenna is λ, and P_{TS} and L_{fwd} are the measured threshold power (the power required to activate the tag) and forward losses, correspondingly [42].

Next, to measure the backscattered signal of the sensor tags, the Thingmagic M6 Reader was used. It was comprised of an RFID reader antenna via a connecting cable, and interfacing software was used. The operation of the reader was maintained at a frequency range of 865.6–867.6 MHz, which is the European standard range for frequency. The power level of the reader antenna was maintained at 28 dBm. The sensor tags were measured within an office environment. The reader was used to measure the backscattered signal strength before and after exposure to a temperature of 50°C.

The measurement of the backscattered signal strength was conducted in two different stages. Firstly, the backscattered signal strength of the sensor tag only was measured. This was done to observe the sensing behaviour of the developed sensor tag. In the second stage, a reference tag was used to measure the relative change in backscattered signal strength. The use of the reference tag enables the sensor tag and reference tag system to be stable. Using the reference tag enables the observation of the relative change in backscattered signal strength values, as apart from the "bending due to the heat" factor, all other factors remain the same for the pair of tags. For the measurement process, the sensor tag was placed at a distance of 50 cm from the M6 reader antenna, as illustrated in Figures 3 and 4.

To measure the backscattered signal strength with the reference tag, it was placed orthogonally at 3 cm apart from the sensor tag, as presented in Figure 5. This was done to enable both tags to be within the same channel of the reader antenna's signal.

For high-temperature exposure sensing, the change in backscattered power from its initial to its bent state was compared using the following equation:

$$\text{dP\%} = \left|\frac{P_{\text{tag}} - P_{\text{ref}}}{P_{\text{ref}}}\right|, \tag{2}$$

where P_{tag} and P_{ref} are the backscattered RSSI power converted from dBm to mW, as explained in [30].

After acquiring the initial readings, the sensor tags were placed within an oven to a temperature of 50°C for about 30 seconds. After exposure to 50°C, the sensor tag bent, as illustrated in Figure 6. After the bending process, the sensor tag was placed in a similar manner as the initial setup, as illustrated in Figures 4 and 5.

3. Results and Discussion

3.1. Thermo Reactive Filament Study. Figure 7 represents the bending behavior of the substrate, whereas Figure 8 represents the microscopic images of the substrate before and after exposure to the oven. The images were taken at both sides of the filament, before and after exposure to 50°C.

The bottom side of the filament, presented in Figure 8, is the layer of the TRF filament that was printed first on Kapton. When removed from Kapton, its surface turned out to be very smooth. The fine lines as seen in the images are the gaps caused during the printing process. Although there has been a significant change in shape based on a visual observation, the microscopic images presented in this segment of the study show few changes within the structural arrangement of the filament after exposure to 50°C. The gaps between the filament lines increased a little, whereas on the top side, the filament appears to have become a bit rougher.

3.2. Sensor Tag Measurement. Initially, the read range measurement of a sensor tag was conducted. Figure 9 represents the change in read range values from its initial state to its bent state, i.e., after exposure to 50°C. The theoretical read range of the sensor tag changed from a maximum value of approximately 8 m to close to 3 m within the UHF range, signifying a reduction of approximately 5 m. As can be seen, in both stages, the sensor tag is functional throughout the global UHF RFID frequency range.

The change in backscattered signal strength from the initial to the bent stage at 50°C is presented in Figure 10. From there, it has been observed that the change in backscattered signal strength from the unbent state to the bent state was approximately −36 dBm to −43 dBm. The observation was quite similar for both sensor tags tested, as shown in Figure 10.

In this segment of the sensor tag evaluation, i.e., the evaluation of the single sensor tag, the significant decrease in the backscattered signal strength from the initial unbent to the bent state is indicative of the sensing behaviour of the tag.

Measurement of a sensor tag paired with a reference tag.

For the measurements with reference tags, two pairs of sensor tags and reference tags were used. The pairs were

(a) (b)

Figure 4: Arrangement of the single sensor tag test: initially (a) and after bending (b).

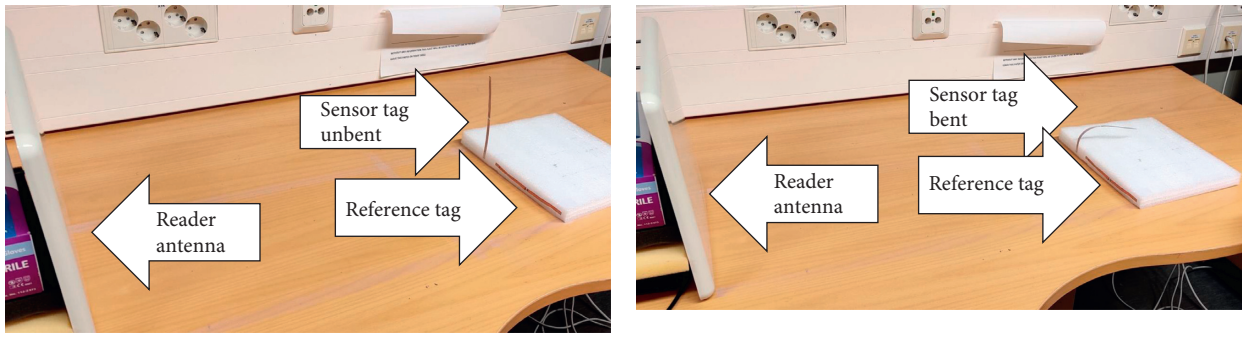

(a) (b)

Figure 5: Arrangement of the sensor tag and reference tag test: unbent sensor tag (a) and bent sensor tag (b).

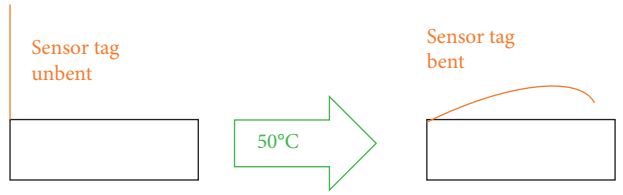

Figure 6: The bending process of the TRF filament and sensor tag from its unbent state to its bent state after exposure to the higher temperature.

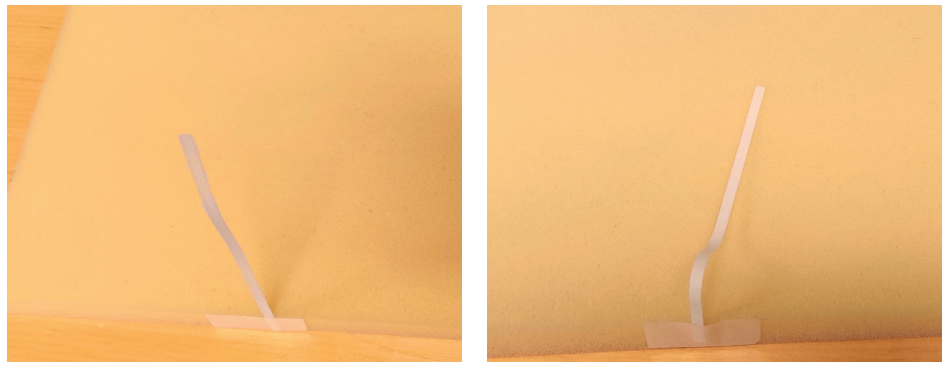

(a) (b)

Figure 7: The developed substrate before exposure to the oven (a) and after exposure to the oven (b).

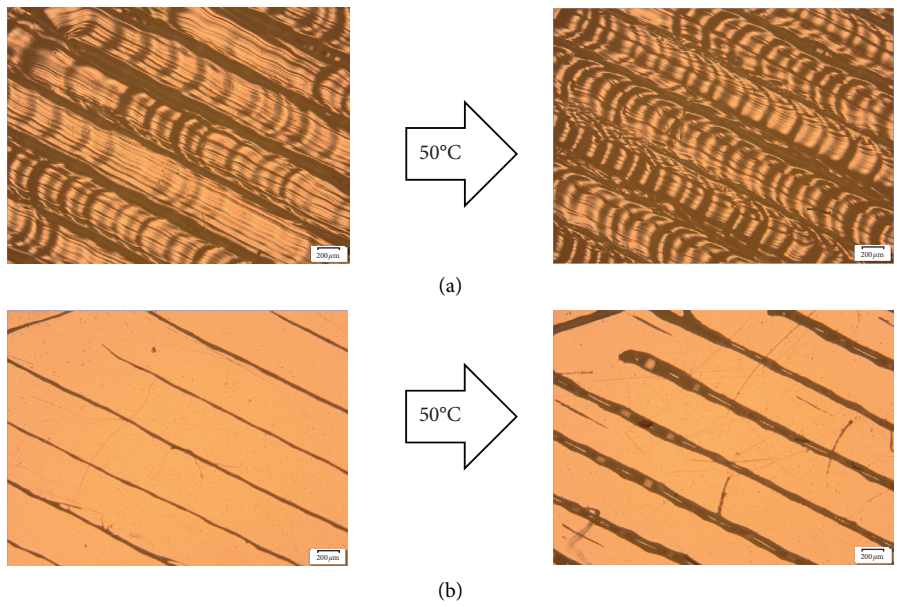

Figure 8: Microscopic images: top side of the filament (a) and bottom side of the filament (b).

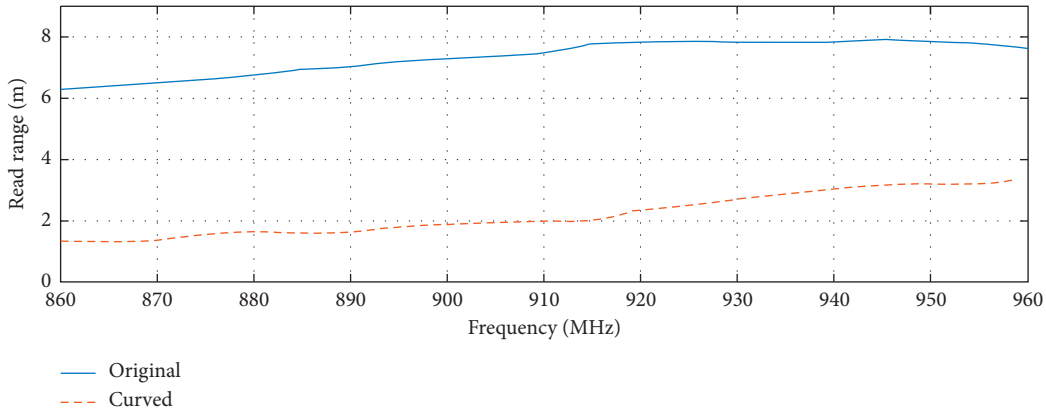

Figure 9: Read range measurements of the sensor tag at the unbent and bent states.

tested initially in the orientation as presented in Figure 4. After the initial measurement, the pairs were placed within the oven at 50°C for 30 seconds. They were then measured for backscattered signal strength after the sensor tag bent.

Figure 11 presents the change in dP% or the relative change in backscattered signal strength before and after exposure to 50°C. In this segment of the backscattered signal strength evaluation, i.e., with the sensor tag and reference tag pair, changes in dP% for both sample pairs were from approximately 30% in the initial state to close to 100% at their bent state, a change of nearly 70%.

Curving of a dipole antenna significantly impacts its performance, as shown also in previous studies [24, 43, 44], and antenna-IC impedance mismatching has been found to make the most effect. This finding also illustrates the sensing behaviour of the sensor tag in this study, when only the factor of "bending due to heat" is considered in the sensing environment. From the experimental observations, it can be determined that the sensor tag presented in this experiment is significantly sensitive to high temperature. The rapid change in shape within a short time frame of 30 seconds could make it an effective sensor for monitoring exposure to high temperatures. There are many applications, where keeping the temperature below a specific maximum temperature is vital, e.g., if a critical product must be kept below a certain temperature during manufacturing, which can be the case for pharmaceutical drugs and food products. Furthermore, there can be a need to alarm about a temperature rise in a certain working environment to maintain safety and comfort. Although the sensor tag is thin and stands steadily also when moved around, as the

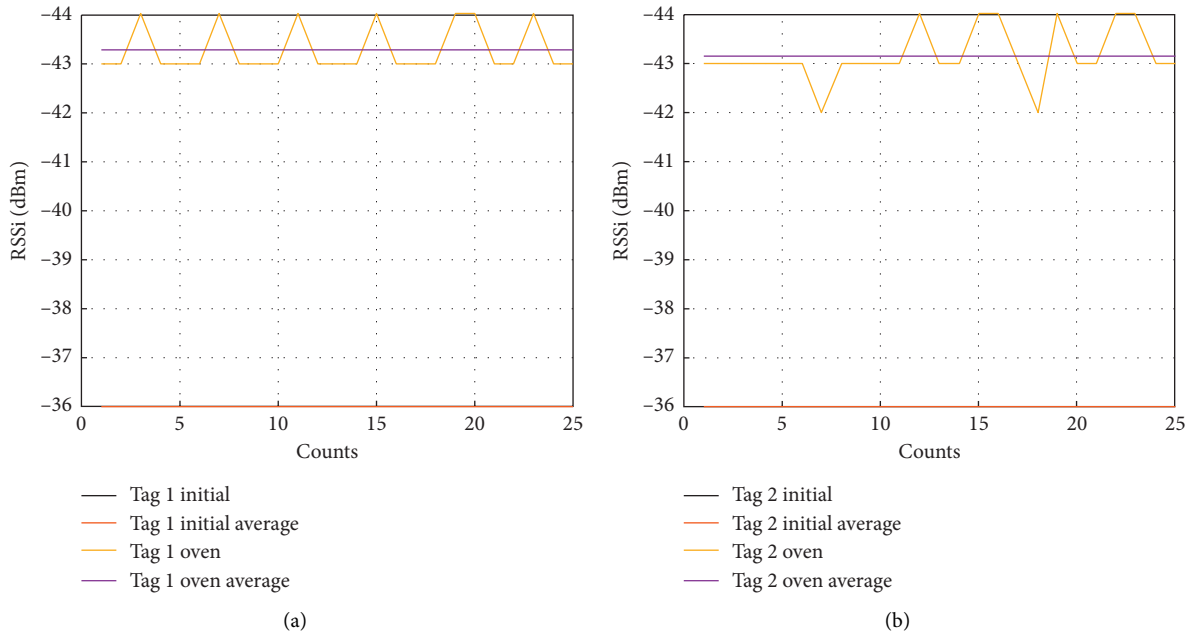

Figure 10: Change in backscattered signal strength during the unbent and subsequent bending states for Tag 1 (a) and Tag 2 (b).

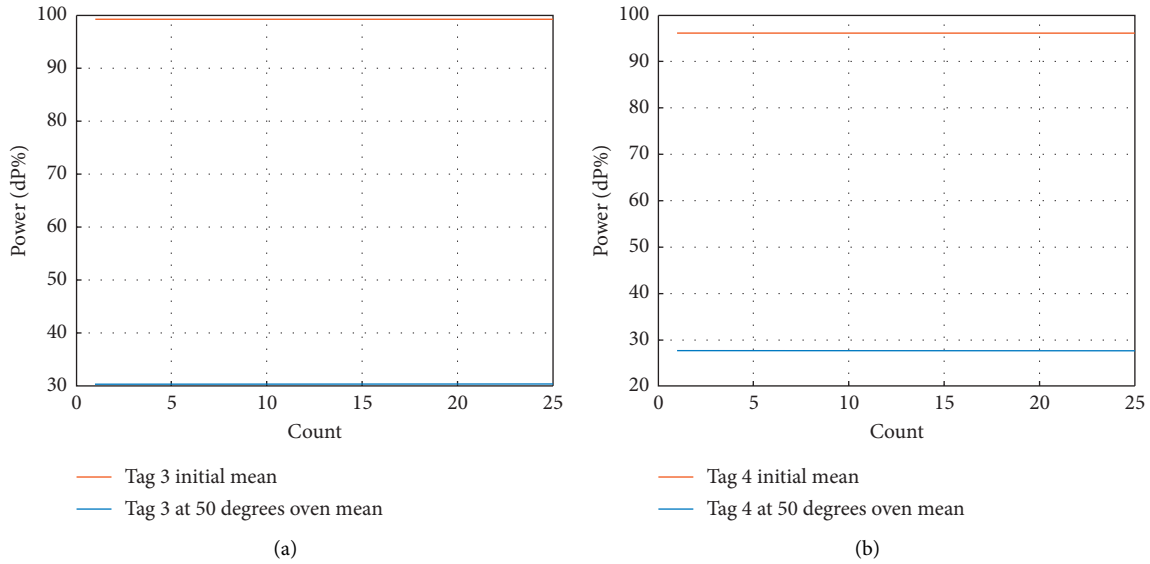

Figure 11: Change in dP% from the initial state to the bent state for Tag 3 (a) and Tag 4 (b).

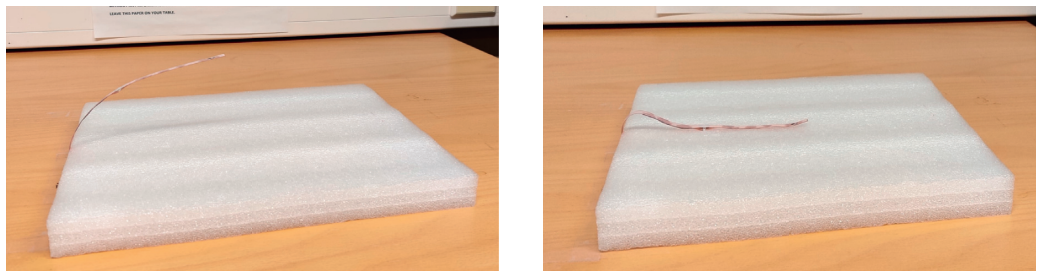

(a) (b)

Figure 12: Continued.

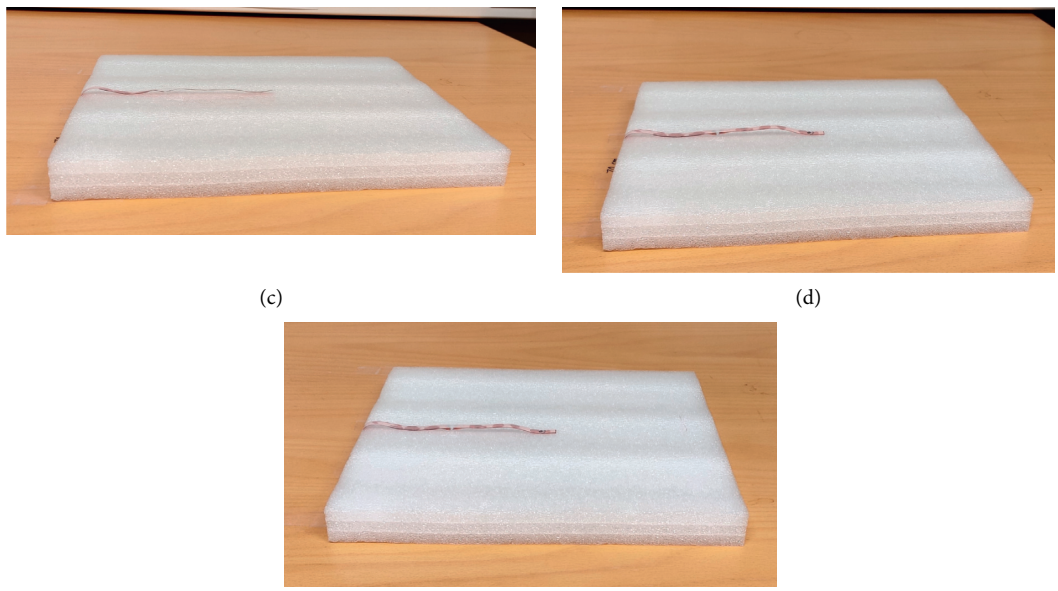

(c) (d)

(e)

Figure 12: Bending of a sensor tag when exposed to different temperatures: 45°C (a), 55°C (b), 60°C (c), 65°C (d), and 70°C (e).

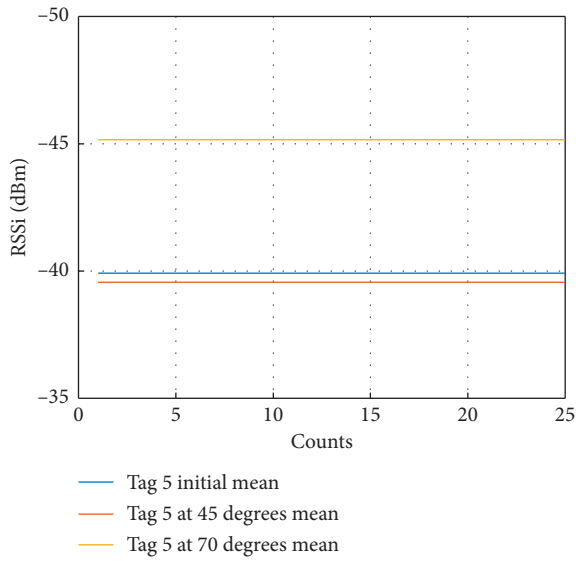

Figure 13: Backscattered signal strength of tag 5 after exposure to different temperatures.

3D-printed layer is firm in a room temperature, this first prototype of the sensor system may not be suitable for environments where the sensor tag would be under harsh vibration or mechanical stresses, which may be the case for example in logistics applications.

3.3. Measurements of Sensor Tags at Different Temperatures. To further evaluate the effects of different temperatures on the sensor tag performance, sensor tags were exposed to the following conditions: 45°C, 55°C, 60°C, 65°C, and 70°C for 30 seconds. As presented in Figure 12, 45°C for 30 seconds did not cause a significant change in the sensor tag shape. The sensor tag was then tested for backscattered signal strength measurement, in a way presented in Figures 4, and Figure 13 presents the change in the backscattered signal strength. As can be seen from Figure 12, the change in the backscattered signal from its initial state is not significant. Thus, exposure to 45°C for 30 seconds did not cause any major change to the sensor tag performance, and it can be considered to be below the threshold temperature of the sensor system.

The sensor tag got fully flat already after 30 seconds in 55°C, and the result is the same in all higher temperatures, as can be seen from Figure 12. When the sensor tag has reached the fully flat condition, it was still working well as a sensor, as can be seen from the backscattered signal strength

measurement results in Figure 13. Thus, we can conclude that the threshold temperature of the developed sensor tag is 50°C, and the sensor system can be used at least up to 70°C.

4. Conclusions

The passive UHF RFID temperature sensor introduced in this study has been evaluated for its wireless performance when exposed to a high temperature. After exposure to a temperature of 50°C for about 30 seconds, there was a decrease in the backscattered signal strength of the sensor tag from −36 dBm to approximately −44 dBm. When compared to a reference tag, the relative backscattered power change varied by about 70%. As the change in the sensor tag shape after being exposed to high temperature is irreversible under normal conditions, the developed system could be developed further for low-cost high-temperature exposure monitoring. Based on these first results, the threshold temperature of the developed sensor tag is 50°C, and the sensor system can be used at least up to 70°C. As the sensor system is fully passive, it is also a maintenance-free and cost-effective alternative for more complex temperature monitoring systems. Future studies will evaluate a more effective use of the proposed design. Some aspects that need to be studied are varying the temperature over a wider range or varying the infill density and the thickness of the thermoconductive filament substrate. Another aspect of future studies is to make the sensor tag antenna more mechanically stable, which will enable a wide variety of new applications for example in logistics.

Data Availability

The data used to support the findings of this study are available from the corresponding author upon request.

Conflicts of Interest

The authors declare that there are no conflicts of interest regarding the publication of this paper.

Acknowledgments

The authors thank Unitika Limited for providing Thermo Reactive Filament used in this experiment. This research has been funded by the Jane and Aatos Erkko Foundation, The Finnish Cultural Foundation and Academy of Finland (decision nos. 294534 and 337861).

References

[1] M. Bolić, D. Simplot-Ryl, and I. Stojmenović, *RFID Systems: Research Trends and Challenges*, Wiley, Hoboken, NJ, USA, 2008.

[2] J. Banks, M. A. Pachano, L. G. Thompson, and D. Hany, *RFID Applied*, Wiley, Hoboken, NJ, USA, 2007.

[3] N. C. Karmakar, J. K. Saha, and E. M. Amin, *Chipless RFID Sensors*, Wiley, Hoboken, NJ, USA, 2008.

[4] F. Deng, Y. He, C. Zhang, and W. Feng, "A CMOS humidity sensor for passive RFID sensing applications," *Sensors*, vol. 14, no. 5, pp. 8728–8739, 2014.

[5] A. Mehmood, H. He, X. Chen et al., "Clothface: a passive RFID-based human-technology interface on a shirtsleeve," *Advances in Human-Computer Interaction*, vol. 2020, Article ID 8854042, 8 pages, 2020.

[6] S. Piramuthu and W. Zhou, *Automation in the Food Industry: Ensuring Quality and Safety Through Supply Chain Visibility*, Wiley-Blackwell, Hoboken, NJ, USA, 2016.

[7] M. M. Islam, K. Rasilainen, and V. Viikari, "Implementation of sensor RFID: carrying sensor information in the modulation frequency," *IEEE Transactions on Microwave Theory and Techniques*, vol. 63, no. 8, pp. 2672–2681, 2015.

[8] E. Perret, R. Frequency Identification, and S. From, *RFID to Chipless RFID*, John Wiley & Sons, Hoboken, NJ, USA, 2014.

[9] S. Caizzone, E. DiGiampaolo, and G. Marrocco, "Wireless crack monitoring by stationary phase measurements from coupled RFID tags," *IEEE Transactions on Antennas and Propagation*, vol. 62, no. 12, pp. 6412–6419, 2014.

[10] S. Lemey, F. Declercq, and H. Rogier, "Textile antennas as hybrid energy-harvesting platforms," *Proceedings of the IEEE*, vol. 102, no. 11, pp. 1833–1857, 2014.

[11] C. Occhiuzzi, S. Cippitelli, and G. Marrocco, "Modeling, design and experimentation of wearable RFID sensor tag," *IEEE Transactions on Antennas and Propagation*, vol. 58, no. 8, pp. 2490–2498, 2010.

[12] C. Occhiuzzi, C. Vallese, S. Amendola, S. Manzari, and G. Marrocco, "NIGHT-care: a passive RFID system for remote monitoring and control of overnight living environment," *Procedia Computer Science*, vol. 32, pp. 190–197, 2014.

[13] T. Kaufmann, D. C. Ranasinghe, M. Zhou, and C. Fumeaux, "Wearable quarter-wave folded microstrip antenna for passive UHF RFID applications," *International Journal of Antennas and Propagation*, vol. 2013, Article ID 129839, 11 pages, 2013.

[14] O. O. Rakibet, C. V. Rumens, J. C. Batchelor, and S. J. Holder, "Epidermal passive RFID strain sensor for assisted technologies," *IEEE Antennas and Wireless Propagation Letters*, vol. 13, pp. 814–817, 2014.

[15] C. Occhiuzzi, C. Paggi, and G. Marrocco, "Passive RFID strain-sensor based on meander-line antennas," *IEEE Transactions on Antennas and Propagation*, vol. 59, no. 12, pp. 4836–4840, 2011.

[16] F. Long, X. D. Zhang, T. Bjorninen et al., "Implementation and wireless readout of passive UHF RFID strain sensor tags based on electro-textile antennas," in *Proccedings of the 9th European Conference on Antennas and Propagation (EuCAP)*, pp. 1–5, Lisbon, Portugal, April 2015.

[17] S. Merilampi, T. Björninen, L. Ukkonen, P. Ruuskanen, and L. Sydänheimo, "Embedded wireless strain sensors based on printed RFID tag," *Sensor Review*, vol. 31, no. 1, pp. 32–40, 2011.

[18] S. Merilampi, T. Björninen, L. Sydänheimo, and L. Ukkonen, "Passive uhf Rfid strain sensor tag for detecting limb movement," *International Journal on Smart Sensing and Intelligent Systems*, vol. 5, no. 2, pp. 315–328, 2012.

[19] X. Chen, L. Ukkonen, and T. Bjorninen, "Passive E-textile UHF RFID-based wireless strain sensors with integrated references," *IEEE Sensors Journal*, vol. 16, no. 22, pp. 7835-7836, 2016.

[20] J. Siden, X. Zeng, T. Unander, A. Koptyug, and H.-E. Nilsson, "Remote moisture sensing utilizing ordinary RFID tags," in *Proceedings of the IEEE*, pp. 308–311, Atlanta, GA, USA, October 2007.

[21] S. Kim, T. Le, M. M. Tentzeris, A. Harrabi, A. Collado, and A. Georgiadis, "An RFID-enabled inkjet-printed soil moisture sensor on paper for "smart" agricultural applications," in

Proceedings of the IEEE, pp. 1507–1510, Valencia, Spain, November 2014.

[22] S. Sajal, Y. Atanasov, B. D. Braaten, V. Marinov, and O. Swenson, "A low cost flexible passive UHF RFID tag for sensing moisture based on antenna polarization," in *Proceedings of the IEEE International Conference on Electro/Information Technology*, pp. 542–545, Milwaukee, WI, USA, June 2014.

[23] E. Sipilä, J. Virkki, L. Sydänheimo, and L. Ukkonen, "Experimental study on brush-painted passive RFID-based humidity sensors embedded into plywood structures," *International Journal of Antennas and Propagation*, vol. 2016, Article ID 1203673, 8 pages, 2016.

[24] X. Chen, H. He, Z. Khan, L. Sydanheimo, L. Ukkonen, and J. Virkki, "Textile-based batteryless moisture sensor," *IEEE Antennas Wireless Propagation Letters*, vol. 19, no. 1, 2020.

[25] A. Faul and J. Naber, "A novel 915 MHz, RFID-based pressure sensor for glaucoma using an electrically small antenna," *Analog Integrated Circuits and Signal Processing*, vol. 85, no. 1, pp. 167–180, 2015.

[26] A. Beriain, I. Rebollo, I. Fernandez, J. F. Sevillano, and R. Berenguer, "A passive UHF RFID pressure sensor tag with a 7.27 bit and 5.47 pJ capacitive sensor interface," in *IEEE/MTT-S International Microwave Symposium Digest*, pp. 1–3, Montreal, Canada, June 2012.

[27] J. Tan, M. Sathyamurthy, A. Rolapp et al., "A fully passive RFID temperature sensor SoC with an accuracy of ±0.4°C (3σ) from 0°C to 125°C," *IEEE Journal of Radio Frequency Identification*, vol. 3, no. 1, pp. 35–45, 2019.

[28] B. Wang, M.-K. Law, A. Bermak, and H. C. Luong, "A passive RFID tag embedded temperature sensor with improved process spreads immunity for a −30°C to 60°C sensing range," *IEEE Transcations on circuits Systems I*, vol. 61, no. 2, pp. 337–346, 2014.

[29] H. Ge, Y. Yao, and J. Yu, "Study on temperature sensitive characteristics of UHF radio frequency identification temperature sensing tag," *Progress in Electromagnetics Research Letters*, vol. 84, pp. 107–113, 2019.

[30] L. Catarinucci and R. Colella, "Design of UHF RFID devices based on 3D-printing technology," in *Proceedings of the 2nd International Multidisciplinary Conference on Computer and Energy Science (SpliTech)*, pp. 1–4, Split, Croatia, July 2017.

[31] S. H. Naushahi, K. Rasilainen, and V. Viikari, "Realization of RFID tag antenna with 3D printing technology," in *Proceedings of the 2016 10th European Conference on Antennas and Propagation, EuCAP 2016*, pp. 1–4, Davos, Switzerland, April 2016.

[32] R. Colella and L. Catarinucci, "Wearable UHF RFID sensor tag in 3D-printing technology for body temperature monitoring," in *Proceedings of the 2018 2nd URSI Atlantic Radio Science Meeting (AT-RASC)*, pp. 1–4, Gran Canaria, Spain, June 2018.

[33] C. A. Spiegel, M. Hippler, A. Münchinger et al., "4D printing at the microscale," *Advanced Functional Materials*, vol. 30, no. 26, Article ID 1907615, 2019.

[34] Q. Ge, A. H. Sakhaei, H. Lee, C. K. Dunn, N. X. Fang, and M. L. Dunn, "Multimaterial 4D printing with tailorable shape memory polymers," *Scientific Reports*, vol. 6, no. 1, Article ID 31110, 2016.

[35] J. E. M. Teoh, J. An, C. K. Chua, M. Lv, V. Krishnasamy, and Y. Liu, "Hierarchically self-morphing structure through 4D printing," *Virtual and Physical Prototyping*, vol. 12, no. 1, pp. 61–68, 2017.

[36] S. Caizzone, C. Occhiuzzi, and G. Marrocco, "Multi-chip RFID antenna integrating shape-memory alloys for detection of thermal thresholds," *IEEE Transactions on Antennas and Propagation*, vol. 59, no. 7, pp. 2488–2494, 2011.

[37] L. Sumana, E. Florence Sundarsingh, and S. Priyadharshini, "Shape memory alloy-based frequency reconfigurable ultra-wideband Antenna for cognitive radio systems," *IEEE transactions on components, Packaging, and Manufacturing Technology*, vol. 11, no. 1, pp. 3–10, 2011.

[38] J. Virtanen, F. Yang, L. Ukkonen, A. Z. Elsherbeni, A. A. Babar, and L. Sydänheimo, "Dual port temperature sensor tag for passive UHF RFID systems," *Sensor Review*, vol. 34, no. 2, pp. 154–169, 2014.

[39] R. Colella, L. Catarinucci, P. Coppola, and L. Tarricone, "Measurement platform for electromagnetic characterization and performance evaluation of UHF RFID tags," *IEEE Transactions on Instrumentation and Measurement*, vol. 65, no. 4, pp. 905–914, 2016.

[40] S. T. Qureshi, T. Bjorninen, and J. Virkki, "Referenced backscattering compression level indicator based on passive UHF RFID tags," in *Proceedings of the IEEE International Conference on RFID Technologies and Applications*, pp. 1–3, Macau, China, September 2018.

[41] E. Moradi, T. Bjorninen, L. Ukkonen, and Y. Rahmat-Samii, "Effects of sewing pattern on the performance of embroidered dipole-type RFID tag antennas," *IEEE Antennas and Wireless Propagation Letters*, vol. 11, pp. 1482–1485, 2012.

[42] Z. Khan, H. He, X. Chen, L. Ukkonen, and J. Virkki, "Protective coating methods for glove-integrated RFID tags-a preliminary study," in *Proceedings of the 14th European Conference on Antennas and Propagation (EuCAP)*, pp. 1–4, Copenhagen, Denmark, March 2020.

[43] X. Zhou and G. Wang, "Study on the influence of curving of tag antennas on performance of RFID system," in *Proceedings of the Asia-Pacific Radio Science Conference, 2004 Proceedings*, pp. 122–125, Qingdao, China, August 2004.

[44] J. Siden, P. Jonsson, T. Olsson, and G. Wang, "Performance degradation of RFID system due to the distortion in RFID tag antenna," in *Proceedings of the 11th International Conference "Microwave and Telecommunication Technology" Conference proceedings (IEEE Cat No 01EX487)*, pp. 371–373, Sevastopol, Ukraine, September 2001.